Preprints of the 19th World Congress
The International Federation of Automatic Control
Cape Town, South Africa. August 24-29, 2014

Coordinated Closed-Curve Path Following Control of Multi-Unicycle in a Time-Invariant Flow Field ⋆

Yang-Yang Chen * **Yu-Ping Tian** * **Ya Zhang** *

* *School of Automation, Southeast University, Nanjing 210096, P.R. China (e-mail: yychen,yptian@seu.edu.cn).*

Abstract: This paper utilizes a dynamic model of unicycles to address the stabilization of formation motion around closed curves in the presence of a time-invariant flow field. It is shown that our previous concentric compression design can be extended to deal with robust coordinated path following control for fighting against the external flow field. Linear acceleration control for each unicycle is added and combined with the rotation control to achieve both temporal and spatial formation in the case of a spatially variable flow, which breaks the restriction of temporally balanced formation relied solely on the angle control in the literature. A potential function is introduced to force each unicycle's speed greater than the magnitude of flow. The theoretical result is proved by a numerical example.

1. INTRODUCTION

Recent advances in control techniques for autonomous vehicles and agile sensor networks bring researchers the dawn to apply a family of sensor-equipped vehicles to execute surveillance (Chong and Kumar [2003]), environmental fields measurement (Leonard et al. [2007], MBARI [2003]), and persistent survey of biological system (ASAP [2006]). In almost any environment, the sensory performance has been severely affected by an external flow field (e.g., ocean current or atmospheric wind). For example, the atmospheric wind can push each unicycle away from its given path and disrupt the relative position of each pair unicycles (that is formation), which leads to reducing the accuracy of data sampling. Nowadays, most existing coordinated path following control protocols (Sepulchre et al. [2007, 2008], Ghabcheloo et al. [2005, 2007], Zhang and Leonard [2007], Zhang et al. [2007], Chen and Tian [2011, 2013a,b]) are derived based on flow-free motion models and thus they often fail to account for the degradation of control performance caused by flow fields. Therefore, it is urgently needed to design a robust coordinated path following control when vehicles suffer an external flow field.

Prior works on robust coordinated path following control (Paley and Petersion [2009], Mellish et al. [2011], Paley et al. [2009]) focus on separating constant-speed particles around a circle under the assumption that the magnitude of the flow is weaker than the particle's speed. An angular velocity algorithm is provided for each particle to stabilize the temporally balanced formation around a circle in a steady, uniform flow field (Paley and Petersion [2009], Mellish et al. [2011]) and then to coordinate UAVs flying around a convex loop in a spatially invariant wind (Paley et al. [2009]). In Paley and Petersion [2009], the authors point out that one relying solely on the angle control cannot maintain the spatial formation (that is the uniform separation around orbits) even in the simplest case of a steady, uniform flow field. This is due to the fact that the external flow leads to the various actual linear speed of the vehicle at the different location even if the vehicle satisfies constant-speed. Since the exact spatial formation is important to the accuracy of data measurements and the (near) optimal sampling trajectory for each vehicle is often planned to be a simple and closed curve (not limited in a circle or a convex loop) (Leonard et al. [2007], MBARI [2003], ASAP [2006]), we discuss coordinated path following control for both temporal and spatial formation motion around a set of closed orbits in an external flow field.

This paper builds upon our prior research on the geometric extension design. The key idea of this approach is to extend the given curve to be a set of level curves of the orbit function for path following and then incorporate the orbit function into the arc-length function to give the solution to formation motion around the given orbits. In the absence of a flow field, coordinated Newtonian particles formation motion around closed curves is solved based on the geometric extension along each curve's normal vector (Zhang and Leonard [2007], Zhang et al. [2007]). To maintain the same geometric topology among the extended curves and the given curve, Chen and Tian propose the concentric compression design to deal with cooperative motion along convex loops at first (Chen and Tian [2011, 2013a]) and then a kind of general non-convex and closed curves (Chen and Tian [2013b]). However, the result of using the geometric extension design for coordinated path following control in the presence of a time-invariant flow field is not established yet.

The main contribution of this paper is that we show that the concentric compression design can be extended to deal with the temporal and spatial formation motion around a family of given closed curves in the presence of a time-invariant flow field, which breaks the restriction of temporally balanced formation on a circle or a convex loop in the literature. The external flow field under consideration is known, nonuniform and time-invariant, which covers the types of the time-invariant flow field considered in the almost results (Paley and Petersion [2009], Mellish et al. [2011], Paley et al. [2009]). The vehicle under consideration is the dynamics of unicycle which is difference from the constant-speed particle (Paley and Petersion [2009], Mellish et al. [2011], Paley et al. [2009]) on the additional linear acceleration control. We first let the inertial velocity of the flow convert to the linear speed and the orientation of the unicycle. Then the component where the linear acceleration and the

⋆ This work was supported by the National Natural Science Foundation of China under grants 61203356, 61273110, 61105113, 61374069 and Doctoral Fund of Ministry of Education of China under grant 20110092120025.

angular acceleration are projected onto the actual orientation of each unicycle is used to accomplish both temporal and spatial formation, at the same time, the component where the linear acceleration and the angular acceleration are projected onto the normal vector perpendicular to the actual orientation of each unicycle is applied to achieve the orbit tracking. For the purposed of ensuring that the magnitude of flow is weaker than each unicycle's speed, a potential function often used in collision avoidance (Chen and Tian [2009]) is introduced into the controller design.

This paper is organized as follows. Section 2 summarizes the unicycle's model in an external flow field and formulates the coordinated control problem based on concentric compression. In Section 3, the control design scheme is designed based on the backstepping technology. Simulation results is given in Section 4. Section 5 provide conclusion.

2. PROBLEM STATEMENT

2.1 Unicycle's model in a time-invariant flow field

In this subsection, we will show the dynamic model of a unicycle in a time-invariant flow field. Each unicycle is subject to two independent control inputs $\{u_i, \tau_i\}$ in order to provide the linear acceleration force and the angular moment in the flow field. Let $\mathbf{z}_i = \left[z_i^x, z_i^y\right]^T \in \mathbb{R}^2$ indicate the position of the wheel axis center defined in an inertia coordinate frame $\mathscr{W}$. Also let θ_i be the ith unicycle's orientation with respect to the x-axis of $\mathscr{W}$. υ_i and ω_i are its linear and angular velocities, respectively. In this paper, the flow field is known and time-invariant. Its inertial velocity at $\mathbf{z}_i$ is represented as $\mathbf{f}(\mathbf{z}_i) = [f^x(\mathbf{z}_i), f^y(\mathbf{z}_i)]^T$ such that $\|\mathbf{f}\| \le f_M < \infty$ where f_M is a bounded constant. With loss of generality, the flow field is permitted to be spatially variable (non-uniform) as long as it is C^2 smooth where $\mathbf{f}' = \partial\mathbf{f}/\partial\mathbf{z}_i = [\nabla f^x, \nabla f^y]^T = \begin{bmatrix} \partial f^x/\partial z_i^x & \partial f^x/\partial z_i^y \\ \partial f^y/\partial z_i^x & \partial f^y/\partial z_i^y \end{bmatrix}$. The dynamics of a unicycle in the presence of a time-invariant flow field is

$$\begin{aligned} \dot{z}_i^x &= \upsilon_i \cos\theta_i + f^x \\ \dot{z}_i^y &= \upsilon_i \sin\theta_i + f^y \\ \dot{\theta}_i &= \omega_i \\ \dot{\upsilon}_i &= u_i \\ \dot{\omega}_i &= \tau_i. \end{aligned} \tag{1}$$

Remark 1. In Mellish et al. [2011], Paley et al. [2009], only a uniform, time-invariant flow so that $\mathbf{f} = [\beta, 0]^T$ is considered where constant β satisfies that $|\beta| < 1$ due to the unit speed of each particle. A simple non-uniform time-invariant flow $\mathbf{f} = \left[f^x(z_i^x), f^y(z_i^y)\right]^T$ is discussed in Paley and Peterson [2009]. Compared with the flow field considered in this paper, each above mentioned flow field (Paley et al. [2009], Mellish et al. [2011], Paley and Petersion [2009]) can be regarded as a special case of this paper.

Let $\gamma_i = \arctan 2(\dot{z}_i^x, \dot{z}_i^y)$ be the orientation of the total inertial velocity of the ith unicycle and $\upsilon_{f_i} = \|\dot{\mathbf{z}}_i + \mathbf{f}\|$ denote its magnitude. Also let $\mathbf{x}_i = [\cos\gamma_i, \sin\gamma_i]^T$ be the unit vector tangent to the trajectory of the ith unicycle at the current location and the normal vector $\mathbf{y}_i$ is perpendicular to $\mathbf{x}_i$. The dynamics of the position of the ith unicycle can be written as $\dot{\mathbf{z}}_i = \upsilon_{f_i}\mathbf{x}_i$. In the following, we first show the dynamics of γ_i. From the first two equations of (1), we have

$$\tan\gamma_i = \frac{\upsilon_i \sin\theta_i + f^y}{\upsilon_i \cos\theta_i + f^x}. \tag{2}$$

Differentiating (2) with respect to time along the solution of (1) for $\dot{\gamma}_i$, we obtain

$$\dot{\gamma}_i = \kappa_{\gamma_i}^u u_i + \kappa_{\gamma_i}^\omega \omega_i + d_{\gamma_i} \tag{3}$$

where $\kappa_{\gamma_i}^u = -\upsilon_i^{-1}\upsilon_{f_i}^{-1}(\mathbf{f}\cdot\mathbf{y}_i)$, $\kappa_{\gamma_i}^\omega = 1 - \upsilon_{f_i}^{-1}(\mathbf{f}\cdot\mathbf{x}_i)$ and $d_{\gamma_i} = (\nabla f^x \cdot \mathbf{x}_i)\cos\gamma_i - (\nabla f^y \cdot \mathbf{x}_i)\sin\gamma_i$.

It is obvious that equation (3) is suitable when $\upsilon_i > \|\mathbf{f}\|$ or $\upsilon_i < \|\mathbf{f}\|$. In this paper, we only consider the situation that $\upsilon_i > \|\mathbf{f}\|$. Next we will express υ_{f_i} as a function of $(\upsilon_i, \mathbf{f}, \gamma_i)$. Also from the first two equations of (1), one gets

$$\upsilon_{f_i} = \sqrt{\upsilon_i^2 - \|\mathbf{f}\|^2 + 2(\mathbf{f}\cdot\mathbf{x}_i)\upsilon_{f_i}} \tag{4}$$

which implies

$$\upsilon_{f_i}^2 - 2(\mathbf{f}\cdot\mathbf{x}_i)\upsilon_{f_i} + \|\mathbf{f}\|^2 - \upsilon_i^2 = 0. \tag{5}$$

When $\upsilon_i > \|\mathbf{f}\|$, the quadratic equation (5) has the solution

$$\upsilon_{f_i} = \mathbf{f}\cdot\mathbf{x}_i + \sqrt{\upsilon_i^2 - (\mathbf{f}\cdot\mathbf{y})^2}. \tag{6}$$

Differentiating (6) with respect to time along the solution of (1) and solving for $\dot{\upsilon}_{f_i}$ using (3), we obtain

$$\dot{\upsilon}_{f_i} = \kappa_{\upsilon_{f_i}}^u u_i + \kappa_{\upsilon_{f_i}}^\omega \omega_i + d_{\upsilon_{f_i}} \tag{7}$$

where $\kappa_{\upsilon_{f_i}}^u = \kappa_{\gamma_i}^u\left[(\mathbf{f}\cdot\mathbf{y}_i) - \left(\upsilon_{f_i} - \mathbf{f}\cdot\mathbf{x}_i\right)^{-1}(\mathbf{f}\cdot\mathbf{y}_i)(\mathbf{f}\cdot\mathbf{x}_i)\right] + (\upsilon_{f_i} - \mathbf{f}\cdot\mathbf{x}_i)^{-1}\upsilon_i$, $\kappa_{\upsilon_{f_i}}^\omega = \kappa_{\gamma_i}^\omega\left[(\mathbf{f}\cdot\mathbf{y}_i) - \left(\upsilon_{f_i} - \mathbf{f}\cdot\mathbf{x}_i\right)^{-1}(\mathbf{f}\cdot\mathbf{y}_i)(\mathbf{f}\cdot\mathbf{x}_i)\right]$ and $d_{\upsilon_{f_i}} = \upsilon_{f_i}(\mathbf{f}'\mathbf{x}_i)\cdot\mathbf{x}_i - \upsilon_{f_i}\left(\upsilon_{f_i} - \mathbf{f}\cdot\mathbf{x}_i\right)^{-1}(\mathbf{f}\cdot\mathbf{y}_i)(\mathbf{f}'\mathbf{x}_i)\cdot\mathbf{y}_i$. In addition, from (5) one gets $\upsilon_i = \sqrt{\upsilon_{f_i}^2 - 2(\mathbf{f}\cdot\mathbf{x}_i)\upsilon_{f_i} + \|\mathbf{f}\|^2}$ and then $\kappa_{\gamma_i}^u$ can be rewritten as $\kappa_{\gamma_i}^u = \upsilon_{f_i}^{-1}(\upsilon_{f_i}^2 - 2(\mathbf{f}\cdot\mathbf{x}_i)\upsilon_{f_i} + \|\mathbf{f}\|^2)^{-\frac{1}{2}}(\mathbf{f}\cdot\mathbf{y}_i)$.

In the section 3, we first regard ω_i as a virtual control and then apply the backsteping technology to design τ_i. By using (3) and (7) to calculate (ω_i, u_i) , it is required

$$\left\| \begin{matrix} \kappa_{\gamma_i}^u & \kappa_{\gamma_i}^\omega \\ \kappa_{\upsilon_{f_i}}^u & \kappa_{\upsilon_{f_i}}^\omega \end{matrix} \right\| \neq 0 \tag{8}$$

which implies

$$\begin{aligned} g_{\kappa_i} = &\sqrt{\upsilon_{f_i}^2 - 2(\mathbf{f}\cdot\mathbf{x}_i)\upsilon_{f_i} + \|\mathbf{f}\|^2}\left(\upsilon_{f_i} - \mathbf{f}\cdot\mathbf{x}_i\right)^{-1} \\ &\times \left(1 - \upsilon_{f_i}^{-1}(\mathbf{f}\cdot\mathbf{x}_i)\right) \neq 0. \end{aligned} \tag{9}$$

(9) is true when $\upsilon_i > \|\mathbf{f}\|$ and the proof is similar to the procedure described in Paley and Petersion [2009].

From the above discussion, the dynamics of unicycle with a time-invariant flow becomes

$$\begin{aligned} \dot{\mathbf{z}}_i &= \upsilon_{f_i}\mathbf{x}_i \\ \dot{\mathbf{x}}_i &= \left(\kappa_{\gamma_i}^u u_i + \kappa_{\gamma_i}^\omega \omega_i + d_{\gamma_i}\right)\mathbf{y}_i \\ \dot{\mathbf{y}}_i &= -\left(\kappa_{\gamma_i}^u u_i + \kappa_{\gamma_i}^\omega \omega_i + d_{\gamma_i}\right)\mathbf{x}_i \\ \dot{\upsilon}_{f_i} &= \kappa_{\upsilon_{f_i}}^u u_i + \kappa_{\upsilon_{f_i}}^\omega \omega_i + d_{\upsilon_{f_i}} \\ \dot{\omega}_i &= \tau_i. \end{aligned} \tag{10}$$

Remark 2. As compared with the model of unit-speed particle in a time-invariant flow field (Mellish et al. [2011]), the dynamic

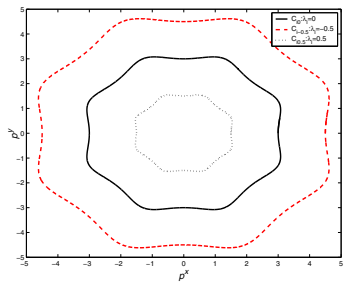

Fig. 1. Concentric compression

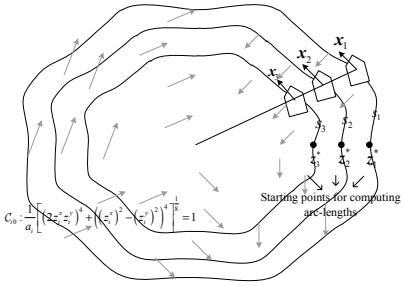

Fig. 2. In-line formation on concentric superellipses

model (10) with the acceleration control is more complex. $\kappa^u_{\upsilon_{f_i}} u_i + \kappa^\omega_{\upsilon_{f_i}} \omega_i$ is the term where the linear acceleration and the angular acceleration are projected onto $\mathbf{x}_i$ and we use it to accomplish the temporal and spatial formation. $\kappa^u_{\gamma_i} u_i + \kappa^\omega_{\gamma_i} \omega_i$ is the component where the linear acceleration and the angular acceleration are projected onto $\mathbf{y}_i$ and it is used to achieve the orbit tracking. In subsection 3.2, these two components are designed at first and then used to solve u_i and ω_i. At last τ_i is obtained by using the backsteping technology.

2.2 Coordinated path following design method

Consider that the given orbit C_{i0} for the ith unicycle is a simple and closed curve with nonzero curvature. Suppose that C_{i0} can be parameterized by using a smooth map $C_{i0} : [0, 2\pi) \to \mathbb{R}^2$, $\phi_i \mapsto C_{i0}(\phi_i)$ with $\|C_{i0}(\phi_i)\| > 0$ and $\|\mathrm{d}C_{i0}(\phi_i)/\mathrm{d}\phi_i\| > 0$, where ϕ_i is the phase angle that describes the direction of the vector from the origin of the orbit to the point on the orbit with respect to the positive axis of the inertial reference frame. Also assume that the vector from the origin of the orbit to the point $\mathbf{z}_{i,k}$ on the orbit and the relative tangent vector to the orbit on $\mathbf{z}_{i,k}$ are linearly independent. Referring to Lemma 1 (Chen and Tian [2013b]), a set of orbits can be obtained by concentric compressing and each one corresponds to a special constant value of the orbit function $\lambda_i(\mathbf{z}_i)$, where $\lambda_i(\mathbf{z}_i)$ satisfies $\nabla\lambda_i(\mathbf{z}_i) \neq 0$ and $|\lambda_i(\mathbf{z}_i)| < \varepsilon_i, (\varepsilon_i > 0)$. The orbit value associated with the given orbit C_{i0} is 0 (see Fig. 1).

To follow the given orbit, the path following control should drive the orbit value $\lambda_i(\mathbf{z}_i)$ and the direction error $\alpha_i \in (-\pi, \pi]$ between the unicycle's motion and the tangent vector to the orbit to 0 asymptotically, i.e.,

$$\lim_{t\to\infty} \lambda_i(\mathbf{z}_i(t)) = 0, \tag{11}$$

$$\lim_{t\to\infty} \alpha_i(t) = 0, \tag{12}$$

Due to the domain of the orbit function, the trajectory of each unicycle should be limited in the set Ω_i, i.e.,

$$|\lambda_i(\mathbf{z}_i(t))| < \varepsilon_i. \tag{13}$$

When each unicycle moves along its given orbit, the control object is to achieve the desired formation with the given orbits adopted. To this end, communication among the unicycles is essential. Let $\mathcal{G} = \{\mathcal{V}, \mathcal{E}\}$ be the bidirectional graph induced by the inter-unicycle communication topology, where $\mathcal{V}$ denotes the set of n unicycles and $\mathcal{E}$ is a set of data links. Also let $\mathcal{N}_i$ denote the neighbor set of the ith unicycle and we assume that $\mathcal{N}_i$ is time-invariant. Two matrices such as the adjacency matrix $A = [a_{ij}]$ and the Lapalacian matrix $L = [l_{ij}]$ are used to represent the graph. The key idea of the formation description on given orbits is based on the consensus design (see fig. 2), which is widely applied in recent works. Some corresponding explanations can be found in Ghabcheloo et al. [2005], Zhang et al. [2007], Chen and Tian [2011, 2013a,b]. It is said that the formation is maintained when the generalized arc-lengths $\xi_i(t)$ defined in Assumption 1 reach consensus and their differentials $\eta_i(t) = \mathrm{d}\xi_i(t)/\mathrm{d}t$ converge to the reference $\eta_*(t)$, i.e.

$$\lim_{t\to\infty} (\xi_i(t) - \xi_j(t)) = 0. \tag{14}$$

$$\lim_{t\to\infty} \eta_i(t) = \eta_*(t). \tag{15}$$

Assumption 1. Each generalized arc-length $\xi_i(s_i(t))$ is a C^2 smooth function of arc-length s_i that $\partial\xi_i/\partial s_i$ satisfies $+\infty > \bar{\varepsilon}_M \geq \frac{\partial\xi_i}{\partial s_i} \geq \bar{\varepsilon}_m > 0$ and that $\partial^2\xi_i/\partial s_i^2$ is uniformly bounded.

In the above subsection, the condition $\upsilon_i > \|\mathbf{f}\|$ is important to deduce the dynamics of unicycle in the flow field. Differing from the assumption that $\upsilon_i > \|\mathbf{f}\|$ (Paley and Petersion [2009], Mellish et al. [2011], Paley et al. [2009]), we design the controller to ensure it in this paper. Because of the relationships between υ_i and the definition of η_i (see (23) in subsection 3.1), here we use

$$\eta_i > \eta^m = 2\bar{\varepsilon}_M f_M \tag{16}$$

to replace $\upsilon_i > \|\mathbf{f}\|$. This is due to the fact that

$$\upsilon_i^2 = \upsilon_{f_i}^2 - 2(\mathbf{f}\cdot x_i)\upsilon_{f_i} + \|\mathbf{f}\|^2 \geq \left(\upsilon_{f_i} - \|\mathbf{f}\|\right)^2 > \|\mathbf{f}\|^2. \tag{17}$$

Assumption 2. The reference $\eta_*(t)$ is uniformly bounded and great than $2\bar{\varepsilon}_M f_M$. Also $\dot{\eta}_*(t)$ is uniformly bounded.

From the above discussion, we define the coordinated path following control problem in a time-invariant flow field as follows:

Coordinated path following problem in a time-invariant flow field: Design a coordinated path following controller

$$\tau_i = g_i\left(\mathbf{z}_i, \upsilon_{f_i}, \gamma_i, \omega_i, u_i, \mathbf{f}, \lambda_i, \alpha_i, \mathbf{x}_i, \mathbf{y}_i, s_i, \xi_i, \xi_j, \eta_*, \dot{\eta}_*\right)$$

$$u_i = \tilde{g}_i\left(\mathbf{z}_i, \upsilon_{f_i}, \gamma_i, \omega_i, \mathbf{f}, \lambda_i, s_i, \xi_i, \eta_i, \xi_j, \eta_j, \eta_*, \dot{\eta}_*\right)$$

for the ith unicycle who suffers a time-invariant flow field $\mathbf{f}$ by using its neighbors' communication information such that requirements (11)-(16) are satisfied.

3. MAIN RESULTS

3.1 Cooperative control model

Let $\mathbf{N}_i = -\frac{\nabla\lambda_i}{\|\nabla\lambda_i\|}$ and $\mathbf{T}_i = \begin{bmatrix} 0 & 1 \\ -1 & 0 \end{bmatrix} \mathbf{N}_i$ be the normal vector and the tangent vector to each level orbit, respectively. The direction error α_i between $\mathbf{x}_i$ and $\mathbf{T}_i$ can be defined as

$$\cos\alpha_i = \mathbf{x}_i \cdot \mathbf{T}_i = \mathbf{y}_i \cdot \mathbf{N}_i, \tag{18a}$$

$$\sin\alpha_i = \mathbf{y}_i \cdot \mathbf{T}_i = -\mathbf{x}_i \cdot \mathbf{N}_i. \tag{18b}$$

The time derivative of (18b) yields

$$\dot{\alpha}_i = \upsilon_{f_i}\left(\kappa_i^a \cos\alpha_i + \kappa_i^b \sin\alpha_i\right) - \left(\kappa_{\gamma_i}^u u_i + \kappa_{\gamma_i}^\omega \omega_i + d_{\gamma_i}\right) \quad (19)$$

where $k_i^a = \frac{1}{\|\nabla\lambda_i\|}\mathbf{T}_i \cdot \nabla^2\lambda_i \mathbf{T}_i$, $k_i^b = -\frac{1}{\|\nabla\lambda_i\|}\mathbf{T}_i \cdot \nabla^2\lambda_i \mathbf{N}_i$ and $\nabla^2\lambda_i$ is the Hessian matrix of $\lambda_i\left(\mathbf{z}_{f_i}\right)$. Since the orbit value with respect to C_{i0} is 0, the position error of path following can be represented as $\lambda_i\left(\mathbf{z}_{f_i}\right)$ and then the dynamics of position error of path following can be written as

$$\dot{\lambda}_i = \nabla\lambda_i \cdot \dot{\mathbf{z}}_i = \upsilon_{f_i}\|\nabla\lambda_i\|\sin\alpha_i. \quad (20)$$

Since the movement of the ith unicycle projected to $\mathbf{T}_i$ leads to the variation in arc-length s_i while the motion along the direction of concentric compression causes the orbit change which also induces the changes of the arc-length, the arc-length s_i measured from the starting point can be written as

$$s_i(\lambda_i, \phi_i) \triangleq \int_{\phi_i^*}^{\phi_i} \frac{\partial s_i(\lambda_i, \tau)}{\partial \tau} d\tau. \quad (21)$$

where the starting points for computing s_i around each level orbit in Ω_i are chose based on the same value of arc-length parameter ϕ_i^* corresponding to the starting point of the given orbit C_{i0}. When the unicycle moves, the variation of generalized arc-length is

$$\dot{\xi}_i = \frac{\partial \xi_i}{\partial s_i}\upsilon_{f_i}\left(\cos\alpha_i + \frac{\partial s_i}{\partial \lambda_i}\|\nabla\lambda_i\|\sin\alpha_i\right). \quad (22)$$

In the next subsection, each unicycle is driven to arrive at its given orbit, which implies $\alpha_i(t) = 0$ and then $\dot{\xi}_i(t) = \frac{\partial \xi_i}{\partial s_i}\upsilon_{f_i}$. In order to reduce the amount of calculation and simplify the design of the control laws, η_i is defined as

$$\eta_i = \frac{\partial \xi_i}{\partial s_i}\upsilon_{f_i}. \quad (23)$$

Then the variation of the generalized arc-length can be written as

$$\dot{\xi}_i = \eta_i + d_{\eta_i} \quad (24)$$

where $d_{\eta_i} = \eta_i\left(-2\sin^2\frac{\alpha_i}{2} + \frac{\partial s_i}{\partial \lambda_i}\|\nabla\lambda_i\|\sin\alpha_i\right)$. Differentiating η_i, we have

$$\dot{\eta}_i = \frac{\partial \xi_i}{\partial s_i}\left(\kappa_{\upsilon_{f_i}}^u u_i + \kappa_{\upsilon_{fi}}^\omega \omega_i + d_{\upsilon_{f_i}}\right) + \frac{\partial^2 \xi_i}{\partial s_i^2}\upsilon_{f_i}(\eta_i + d_{\eta_i}). \quad (25)$$

3.2 Controller design

Step1. Convergence of $\lambda_i, \alpha_i, \xi_i - \xi_j, \eta_i - \eta_*$: The control Lyapunov function is selected as follows:

$$V_I = \sum_{i=1}^n h_i(\lambda_i) - \sum_{i=1}^n \ln\left(\cos\frac{\alpha_i}{2}\right) + \frac{k_0}{4}\sum_{i=1}^n\sum_{j=1}^n a_{ij}(\xi_i - \xi_j)^2 + \sum_{i=1}^n\left(\ln\left(\frac{\eta_i - \eta^m}{\eta_* - \eta^m}\right) + \frac{\eta_* - \eta^m}{\eta_i - \eta^m} - 1\right) \quad (26)$$

where $k_0 > 0$ and $h_i(\lambda_i)$ is a C^2 smooth, nonnegative function on $(-\varepsilon_i, \varepsilon_i)$. Let $h_i(\lambda_i)$ and $\nabla h_i = \mathrm{d}h_i/\mathrm{d}\lambda_i$ satisfy the following conditions:

(C1) $h_i(\lambda_i) \to +\infty$ and $\nabla h_i \to -\infty$ as $\lambda_i \to -\varepsilon_i$.
(C2) $h_i(\lambda_i) \to +\infty$ and $\nabla h_i \to +\infty$ as $\lambda_i \to \varepsilon_i$.
(C3) $h_i(\lambda_i) = 0$ if and only if $\lambda_i = 0$.

In the function (26), the first term contributes to forcing the trajectory of each unicycle to its given orbit and stay in Ω_i when it start from Ω_i. It vanishes when $\lambda_i = 0$. The second term aligns the direction of each unicycle's motion and the tangent vector to the orbit. It vanishes when $\alpha_i = 0$. The next term ensures the consensus of the generalized arc-lengths. It vanishes when $\xi_i = \xi_j$. The fourth term guarantees η_i converge to the reference and $\upsilon_i > \|\mathbf{f}_i\|$ for all time. It vanishes when $\eta_i = \eta_*$.

The time derivation of V_I is

$$\dot{V}_I = \sum_{i=1}^n \tan\frac{\alpha_i}{2}\left(\Delta_{\alpha_i} - \left(\kappa_{\gamma_i}^u u_i + \kappa_{\gamma_i}^\omega \omega_i + d_{\gamma_i}\right)\right) + \sum_{i=1}^n(\eta_i - \eta_*) \times \left((\eta_i - \eta^m)^{-2}\frac{\partial \xi_i}{\partial s_i}\left(\kappa_{\upsilon_{f_i}}^u u_i + \kappa_{\upsilon_{f_i}}^\omega \omega_i + d_{\upsilon_{f_i}}\right) + \Delta_{\eta_i}\right) \quad (27)$$

where

$$\Delta_{\alpha_i} = \upsilon_{f_i}\left(\kappa_i^a\cos\alpha_i + \kappa_i^b\sin\alpha_i\right) + 2\upsilon_{f_i}\nabla h_i\|\nabla\lambda_i\|\cos^2\frac{\alpha_i}{2} + k_0\eta_i\left(-\sin\alpha_i + 2\frac{\partial s_i}{\partial\lambda_i}\|\nabla\lambda_i\|\cos^2\frac{\alpha_i}{2}\right)\sum_{j=1}^n a_{ij}(\xi_i - \xi_j),$$

$$\Delta_{\eta_i} = (\eta_* - \eta^m)^{-2}\frac{\partial^2\xi_i}{\partial s_i^2}\upsilon_{f_i}(\eta_i + d_{\eta_i}) + k_0\sum_{j=1}^n a_{ij}(\xi_i - \xi_j) - (\eta_i - \eta^m)^{-1}(\eta_* - \eta^m)^{-1}\dot{\eta}_*.$$

Here we first use the unicycle's angular velocity ω_i as the virtual control $\bar{\omega}_i$ and the acceleration input u_i to fulfill the coordinated path following control problem. The choices are

$$\begin{bmatrix} \kappa_{\gamma_i}^u & \kappa_{\gamma_i}^\omega \\ \kappa_{\upsilon_{f_i}}^u & \kappa_{\upsilon_{f_i}}^\omega \end{bmatrix}\begin{bmatrix} u_i \\ \bar{\omega}_i \end{bmatrix} = \begin{bmatrix} g_{\alpha_i} \\ g_{\eta_i} \end{bmatrix} \quad (28)$$

where

$$g_{\alpha_i} = \Delta_{\alpha_i} + k_1\sin\frac{\alpha_i}{2} - d_{\gamma_i},$$

$$g_{\eta_i} = -(\eta_i - \eta^m)^2\left(\frac{\partial\xi_i}{\partial s_i}\right)^{-1}(\Delta_{\eta_i} + k_2(\eta_i - \eta_*) + k_3\sum_{j=1}^n a_{ij}(\eta_i - \eta_j)) - d_{\upsilon_{f_i}}.$$

Obviously, equation (28) has a unique solution

$$u_i = g_{\kappa_i}^{-1}\left(\kappa_{\gamma_i}^u g_{\alpha_i} - \kappa_{\upsilon_{fi}}^u g_{\eta_i}\right), \quad (29)$$

$$\bar{\omega}_i = g_{\kappa_i}^{-1}\left(\kappa_{\upsilon_{fi}}^\omega g_{\alpha_i} - \kappa_{\gamma_i}^\omega g_{\eta_i}\right). \quad (30)$$

Remark 4. Since the speed of particle in Paley and Petersion [2009], Mellish et al. [2011], Paley et al. [2009] is fixed (that is, unit-speed), the authors just assume that the flow field satisfies $\|\mathbf{f}\| < 1$. In this paper, the speed is controllable for the purpose of guaranteeing the speed great than $\|\mathbf{f}\|$. To this end, a potential function used in collision avoidance (Chen and Tian [2009]) is introduced in this paper, which can be found in the last term in (26).

Remark 5. In the flow field, the virtual control $\bar{\omega}_i$ and the acceleration input u_i work together to achieve path following and formation motion, while they are separatively responsible for path following and formation motion in Chen and Tian [2011]. All these changes are due to the effect of the external flow field.

Now, substituting (29) and (30) into (27) results in

$$\dot{V}_I = -k_1 \sum_{i=1}^{n} \frac{\sin^2 \frac{\alpha_i}{2}}{\cos \frac{\alpha_i}{2}} - k_2 \sum_{i=1}^{n} (\eta_i - \eta_*)^2$$
$$-k_3 (\eta - \eta_* \mathbf{1}_n)^T L (\eta - \eta_* \mathbf{1}_n) \leq 0 \quad (31)$$

where $\eta = [\eta_1, \ldots, \eta_n]^T$ and $\mathbf{1}_n = [1, \ldots, 1]^T$.

To accomplish the control input τ_i, the error variable is introduced such as

$$\omega_{e_i} = \omega_i - \bar{\omega}_i \quad (32)$$

which should be driven to zero, and re-write $\dot{V}_I$ as

$$\dot{V}_I = -k_1 \sum_{i=1}^{n} \frac{\sin^2 \frac{\alpha_i}{2}}{\cos \frac{\alpha_i}{2}} - k_2 \sum_{i=1}^{n} (\eta_i - \eta_*)^2$$
$$-k_3 (\eta - \eta_* \mathbf{1}_n)^T L (\eta - \eta_* \mathbf{1}_n) + \sum_{i=1}^{n} \omega_{e_i} \Delta_{e_i} \quad (33)$$

where

$$\Delta_{e_i} = -\kappa_{\gamma_i}^{\omega} \tan \frac{\alpha_i}{2} + \kappa_{\upsilon_{f_i}}^{\omega} \frac{\partial \xi_i}{\partial s_i} (\eta_i - \eta^m)^{-2} (\eta_i - \eta_*).$$

Step2. Backstepping for ω_{e_i}: The second control Lyapunov function is given by

$$V_{II} = V_I + \sum_{i=1}^{n} \omega_{e_i}^2. \quad (34)$$

Taking the time derivative of both sides of equation (34) along the solution of (29), one gets

$$\dot{V}_{II} = -k_1 \sum_{i=1}^{n} \frac{\sin^2 \frac{\alpha_i}{2}}{\cos \frac{\alpha_i}{2}} - k_2 \sum_{i=1}^{n} (\eta_i - \eta_*)^2$$
$$-k_3 (\eta - \eta_* \mathbf{1}_n)^T L (\eta - \eta_* \mathbf{1}_n) + \sum_{i=1}^{n} \omega_{e_i} \left(\tau_i - \dot{\bar{\omega}}_i - \Delta_{e_i}\right). \quad (35)$$

We design the yaw force τ_i as follows:

$$\tau_{r_i} = \dot{\bar{\omega}}_i + \Delta_{e_i} - k_4 \omega_{e_i} \quad (36)$$

where $k_4 > 0$, which yields

$$\dot{V}_{II} = -k_1 \sum_{i=1}^{n} \frac{\sin^2 \frac{\alpha_i}{2}}{\cos \frac{\alpha_i}{2}} - k_2 \sum_{i=1}^{n} (\eta_i - \eta_*)^2$$
$$-k_3 (\eta - \eta_* \mathbf{1}_n)^T L (\eta - \eta_* \mathbf{1}_n) - k_4 \sum_{i=1}^{n} \omega_{e_i}^2 \leq 0. \quad (37)$$

3.3 Stability analysis

Under the control laws (29) and (36), the equation of the closed-loop system for λ_i is denoted as (20), the equation of the closed-loop system for α_i is (19) where $\dot{\omega}_i$ satisfies (30) , the equation of the closed-loop system for the relative generalized arc-length is

$$\dot{\xi}_i - \dot{\xi}_j = \eta_i + d_{\eta_i} - \eta_j - d_{\eta_j}, \quad (38)$$

the equation of the closed-loop system for $\eta_i - \eta_*$ satisfies

$$\dot{\eta}_i - \dot{\eta}_* = \left(\frac{\eta_i - \eta^m}{\eta_* - \eta^m} - 1\right) \dot{\eta}_* - (\eta_i - \eta^m)^2 \left(k_0 \sum_{j=1}^{n} a_{ij} (\xi_i - \xi_j)\right.$$
$$\left. + k_2 (\eta_i - \eta_*) + k_3 \sum_{j=1}^{n} a_{ij} (\eta_i - \eta_j)\right). \quad (39)$$

Theorem 1. Consider a family of level closed curves of the orbit function constructed by concentric compression. Suppose the generalized arc-lengths and the reference $\eta^*(t)$ satisfy Assumption 1 and Assumption 2, respectively. Assume the initial conditions of unicycles make the initial value of V_{II} given in (34) finite. Then the coordinated path following control problem in a time-invariant flow field is solved via the linear acceleration force (29) and the angular acceleration force (36) if the communication topology is connected.

Proof. The set $\Phi = \left\{(\lambda_i, \alpha_i, \xi_i - \xi_j, \eta_i - \eta_*, \omega_{e_i}) \,|V_{II} \leqslant c\right\}$ such that $V_{II} \leq c$, for $c > 0$, is closed by continuity. Since $|\lambda_i| < \varepsilon_i$ due to the boundedness of V_{II}, α_i is defined in $(-\pi, \pi]$, $\left|\xi_i - \xi_j\right| \leq \sqrt{4c}$, and $|\eta_i| \leq h_{\eta_i}^{-1}(c) + \eta_* + \eta^m$ where $h_{\eta_i} = \ln\left((\eta_i - \eta^m)/(\eta_* - \eta^m)\right) + (\eta_i - \eta^m)/(\eta_* - \eta^m) - 1$, the set Φ is compact. On the compact set Φ, $\left|\partial s_i(\lambda_i, \phi_i)/\partial \lambda_i\right|$ and $\left|\partial^2 s_i(\lambda_i, \phi_i)/\partial \lambda_i^2\right|$ are bounded because $\phi_i \in [0, 2\pi)$. $\|\nabla \lambda_i\|$ is bounded by continuity. Since $\partial \xi_i / \partial s_i$ is bounded away from 0, $\upsilon_{f_i} = \left(\frac{\partial \xi_i}{\partial s_i}\right)^{-1} \eta_i$ is also bounded on Φ. Thus the closed-loop system is Lipschitz continuous on the set Φ and a solution exists and is unique.

Since the value of V_{II} is time-independent and non-increasing, we conclude that the entire solution stays in Φ and then $\eta_i > \eta^m$ when the initial value of V_{II} is finite,. At the same time, $|\lambda_i(\mathbf{z}_i(t))| < \varepsilon_i$ is satisfied by (C1) and (C2). Applying the invariance-like theorem, it follows that as $t \to \infty$, the trajectories of the closed-loop system will converge to the set inside the region $E = \left\{(\lambda_i, \alpha_i, \xi_i - \xi_j, \eta_i - \eta_*, \omega_{e_i}) \,\middle|\, \dot{V}_{II} = 0\right\}$, that is

$$\alpha_i = 0,\ \eta_i = \eta_*,\ \omega_{e_i} = 0, \quad (40a)$$

$$(\eta - \eta_* \mathbf{1}_n)^T L (\eta - \eta_* \mathbf{1}_n) = 0 \Rightarrow \eta_i = \eta_j. \quad (40b)$$

On the set E, the equations of the whole closed-loop system become

$$\dot{\lambda}_i = 0, \quad (41a)$$

$$\dot{\alpha}_i = -2\upsilon_{f_i} \nabla h_i \|\nabla \lambda_i\| - 2k_0 \eta_i \frac{\partial s_i}{\partial \lambda_i} \|\nabla \lambda_i\| \sum_{j=1}^{n} a_{ij} (\xi_i - \xi_j), \quad (41b)$$

$$\dot{\xi}_i - \dot{\xi}_j = 0, \quad (41c)$$

$$\dot{\eta}_i - \dot{\eta}_* = -k_0 (\eta_i - \eta^m)^2 \sum_{j=1}^{n} a_{ij} (\xi_i - \xi_j). \quad (41d)$$

In the following, we will show $\xi_i - \xi_j \to 0$ as $t \to \infty$. On the set E, from (41c) one gets that $\xi_i - \xi_j$ is constant. Applying the extension of the Barbalat lemma in Micaelli and Samson [1993], from (41d) and Assumption 2, we have $\dot{\eta}_i - \dot{\eta}_* = -k_0 (\eta_i - \eta^m)^2 \sum_{j=1}^{n} a_{ij} (\xi_i - \xi_j) \to 0$. Since $\eta_i - \eta^m \to \eta_* - \eta^m \neq 0$ as $t \to \infty$, one gets $L\xi = 0$ where $\xi = [\xi_1, \ldots, \xi_n]^T$, which implies that $\xi_i - \xi_j \to 0$ as $t \to \infty$ when the communication topology is connected.

Because $\xi_i - \xi_j \to 0$ as $t \to \infty$, the equation of the closed-loop system for α_i on the set E is changed to

$$\dot{\alpha}_i = -2\upsilon_{f_i} \nabla h_i \|\nabla \lambda_i\|. \quad (42)$$

It is easy to check that $\lim_{t \to \infty} \upsilon_{f_i} = (\partial \xi / \partial s_i) \eta_* > 0$ is uniformly continuous and bounded from Assumption 1 and 2. The details can be found in Chen and Tian [2011]. From (41a), λ_i tends to a constant and thus ∇h_i tends to a constant. Therefore, $-2\nabla h_i \upsilon_{f_i} \|\nabla \lambda_i\|$ is uniformly continuous. Applying the extension of the Barbalat lemma Micaelli and Samson [1993], from (42) we have $\dot{\alpha}_i \to 0$ as $t \to \infty$. Because $\lim_{t \to \infty} \upsilon_{f_i} \|\nabla \lambda_i\| \neq 0$, one gets $\nabla h_i \to 0$ as $t \to \infty$. By (C3), λ_i tends to 0.

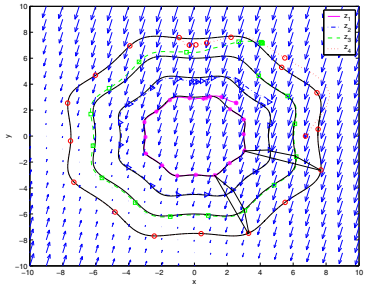

(a) Plot of movements

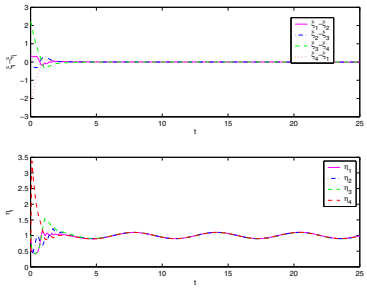

(b) Plots of $\xi_i - \xi_j$ and η_i

Fig. 3. Trapezoidal formation on concentric superellipses

4. SIMULATION RESULTS

The given orbits are a set of concentric superellipses such as $\frac{1}{a_i}\left[\left(2z_i^x z_i^y\right)^4 + \left(\left(z_i^x\right)^2 - \left(z_i^y\right)^2\right)^4\right]^{\frac{1}{8}} = 1$ where $a_i = 3 + 0.5\,(i-1)$, $i = 1,\ldots,4$. In this case, the neighbors of each ship is that $\mathcal{N}_1 = \{\mathcal{V}_2, \mathcal{V}_3\}$, $\mathcal{N}_2 = \{\mathcal{V}_1, \mathcal{V}_3, \mathcal{V}_4\}$, $\mathcal{N}_3 = \{\mathcal{V}_1, \mathcal{V}_2\}$, $\mathcal{N}_4 = \{\mathcal{V}_2,\}$. The desired pattern is that forming a trapezoidal formation with $\eta_* = 1.0 + 0.1\sin(t)$. The starting points are defined as the intersection of the orbits with the positive horizontal axis of $\mathcal{W}$ and we choose $\xi_j = s_j/a_j; (j = 1,4)$, $\xi_2 = s_2/a_2 + \pi/6$ and $\xi_3 = s_3/a_3 + \pi/8$. The control gains are selected as $k_0 = 20, k_j = 10, j = 1,\ldots,5$ and the non-uniform flow field is $\mathbf{f} = [-0.25 * \sin(2\pi * 5/360 * (z_i^x + z_i^y)), 0.25 * \cos(2\pi * 5/360 * (z_i^x + z_i^y))]^T$. The movement of unicycles is shown in Fig. 3(a). From this figure, we can see that four unicycles finally move along the set of given orbits and form the desired formation. Fig. 3(b) demonstrates that ξ_i reaches consensus and η_i converges to the reference. According to these pictures, the coordinated path following control problem in a time-invariant flow field is solved via our proposed controller.

5. CONCLUSION

In this paper, our previous geometric extension design (Chen and Tian [2011]) is developed to deal with coordinated path following control of unicycles in an external time-invariant flow field. Both temporal and spatial formation is achieved by introducing the acceleration control. The potential function is used to force each unicycle's speed greater than the magnitude of flow. The validity of the proposed approach is confirmed by theoretical analysis and numerical simulation.

REFERENCES

C. Chong and S.P. Kumar. Sensor networks: evolution, opportunities, and challenges. *Proceeding of the IEEE*, 91:1247–1256, 2003.

N.E. Leonard, D.A. Paley, F. Lekien, R. Sepulchre, D.M. Frantantoni, R.E. Davis. Collective motion, sensor networks, and ocean sampling. *Proceedings of the IEEE*, 95:48–74, 2007.

MBARI. Autonomous ocean sampling network [Online]. *http://www. mbari.org/aosn/NontereyBay2003/*, 2003.

Princeton University. Adaptive Sampling and Prediction [Online]. *http://www. princeton.edu/ dcsl/asap/*, 2006.

R. Sepulchre, D.A. Paley, and N.E. Leonard. Stabilization of planar collective motion: All-to-all communication. *IEEE Transactions on Automatic Control*, 52:811–824, 2007.

R. Sepulchre, N.E. Leonard, and D.A. Paley. Stabilization of symmetric formations to motion around convex loops. *Syst. Contr. Lett.*, 57:209–215, 2008.

R. Ghabcheloo, A. Pascoal, C. Silvestre, and I. Kaminer. Coordinated path following control of multiple wheeled robots with directed communication links. *Proceedings of the 44th IEEE Conference on Decision and Control, and the European Control Conference*, Seville, Spain, December 7084-7089, 2005.

R. Ghabcheloo, A. Pascoal, C. Silvestre, and I. Kaminer. Nonlinear coordinated path following control of multiple wheeled robots with bidirectional communication constraints. *International Journal of Adaptive Control and Signal Processing*, 21:–3 133–137, 2007.

F. Zhang and N.E. Leonard. Coordinated patterns of unit speed particles on a closed curve. *Syst. Contr. Lett.*, 56:397–407, 2007.

F. Zhang, D.M. Fratantoni, D.A. Paley, J. Lund, N.E. Leonard. Control of coordinated patterns for ocean sampling. *International Journal of Control*, 80:1186–1199, 2007.

Y.-Y. Chen and Y.-P. Tian. A curve extension design for coordinated path following control of unicycles along given convex loops. *International Journal of Control*, 84:1729–1745, 2011.

Y.-Y. Chen and Y.-P. Tian. Coordinated adaptive control for 3D formation tracking with a time-varying orbital velocity. *IET Control Theory Appl.*, 7:646–662, 2013.

Y.-Y. Chen and Y.-P. Tian. Coordinated adaptive control for formation tracking surface vessels with a time-invariant orbital velocity. *Proceedings of 32nd Chinese Control Conference*, Xian, China, 7445–7450, 2013.

D.A. Paley and C. Petersion. Stabilization of collective motion in a time-invariant flow field. *AIAA J. Guidance, Control, and Dynamics*, 32:771–779, 2009.

R. Mellish, S. Napora, and D.A. Paley. Backstepping control design for motion coordination of self-propelled vehicles in a flowfield. *International Journal of Robust and Nonlinear Control*, 21:1452-1466, 2011.

D.A. Paley, L. Techy, and C.A. Woolsey. Coordinated perimeter patrol with minimum-time alert response. *AIAA J. Guidance, Navigation, and Control Conference and Exhibit*, Chicago, IL, United states, 2009-6210, 2009.

E.W. Weisstein. Superellipse [Online]. *http://mathworld.wolfram.com/Superellipse.html*.

Y.-Y. Chen and Y.-P. Tian. A backstepping design for directed formation control of three-coleader agents in the plane. *Int. J. of Robust and Nonlinear Control*, 9:729–745, 2009.

A. Micaelli, C. Samson. Trajectory tracking for unicycle-type and two-steering-wheels mobile robots. *INRIA report 2097*, 1993.